

# Study of the Pulsar Wind Nebula HESS J1857+026 with Fermi-LAT

R. Rousseau, M.-H. Grondin, A. Van-Etten, M. Lemoine-Goumard, C. Espinoza, A. Lyne, D. Smith, B. Stappers, and (J.-M. Casandjian)

(Affiliations can be found after the references)

Received / Accepted

## ABSTRACT

**Context.** Since its launch in June 2008, the Fermi satellite has firmly identified 5 pulsar wind nebulae plus a large number of candidates, all powered by young and energetic pulsars. HESS J1857+026 is an extended gamma-ray source detected by H.E.S.S. during the Galactic Plane Survey and identified as the pulsar wind nebula powered by the pulsar PSR J1856+0245.

**Aims.** We search for gamma pulsations from the pulsar PSR J1856+0245 and explore the characteristics of its associated pulsar wind nebula.

**Methods.** Using a rotational ephemeris obtained with 76 observations made with the Jodrell Bank Telescope at 1.520 GHz, we phase-fold 31 months of gamma-ray data acquired by the Large Area Telescope aboard Fermi. We also perform a complete  $\gamma$ -ray spectral and morphological analysis.

**Results.** No pulsation is detected from PSR J1856+0245. However, significant emission is detected above 5 GeV at a position coincident with the TeV source HESS J1857+026. The gamma-ray spectrum is well described by a simple power law with a spectral index of  $\Gamma = 1.52 \pm 0.16 \pm 0.55$  and an energy flux of  $G(100 \text{ MeV} - 100 \text{ GeV}) = (2.72 \pm 0.58 \pm 1.51) \times 10^{-11} \text{ ergs/cm}^2/\text{s}$ . This yields a  $\gamma$ -ray efficiency of  $\sim 5\%$ , in the range expected for pulsar wind nebulae. Detailed multi-wavelength modeling brings new constraints on the energetics and magnetic field of the pulsar wind nebula system.

**Key words.** Pulsar Wind Nebula - Plerion - Fermi-LAT - Gamma-Ray - HESS J1857+026 - PSR J1856+0245

## 1. Introduction

The dissipation of the rotational energy of a pulsar leads to the creation of a relativistic wind made of electron/positron pairs. This inflating magnetized wind drives a shock and expands until its pressure is balanced by that of the surrounding medium, which is often a Supernova Remnant (SNR) (Gaensler et al. 2006). This phenomenon creates a Pulsar Wind Nebula (PWN).

Since 2003, the continuous observations of the Galactic Plane by Čerenkov telescopes (especially HESS<sup>1</sup> but also VERITAS and MAGIC) have yielded the detection of more than 60 Galactic sources. Among them, PWN is the dominant class with 28 sources firmly identified. In the GeV energy range, 5 PWNe have been firmly identified using Fermi-LAT data. All are powered by energetic pulsars and their  $\gamma$ -efficiencies are  $\sim 1\%$  consistent with TeV observations by HESS (Ackermann et al. 2011; Grondin et al. 2011a). Furthermore Fermi-LAT has detected an increasing population of pulsars (96) as well as new PWNe candidates and provides new constraints on radiation processes (Abdo et al. 2010a; Pellizzoni et al. 2010).

The presence of a pulsar close to the source position is an important clue to confirm the identification of a PWN, which often requires information from the radio/X-ray wavelengths. The radio/X-ray PWNe are often associated with TeV extended sources slightly offset from their pulsars. This offset can be explained by taking into account the inhomogeneous environment leading, for instance, to an asymmetric PWN (Hinton et al. 2010). In such sources, TeV radiation can be explained by Inverse Compton (IC) scattering of an old population of leptons produced earlier in the pulsar's life on ambient photon fields (CMB, IR, ...) or by  $\pi^0$  decay from the interaction of accelerated hadrons with nuclei of the interstellar medium.

HESS J1857+026 is a very high energy (VHE) gamma-ray source detected by HESS during the Galactic Plane Survey (Aharonian et al. 2008) and later detected by MAGIC (Klepser et al. 2011). The extended ( $\sim 0.11^\circ$ ) TeV source was identified as a PWN after the discovery of PSR J1856+0245 (offset  $\sim 0.12^\circ$ ) in the Arecibo PALFA survey (Hessels et al. 2008). PSR J1856+0245 is an energetic pulsar ( $\dot{E} = 4.6 \times 10^{36} \text{ erg/s}$ ) located in a dense region,  $1.3^\circ$  from the bright SNR W44 (Abdo et al., 2010) and  $0.6^\circ$  from the fainter SNR HESS J1858+020 on which only an upperlimit could be set using Fermi data (Torres et al. 2011). Interestingly, significant emission coincident with HESS J1857+026 was observed above 100 GeV using Fermi-LAT data (Neronov et al. 2010).

Here, we report in details GeV observations of the HESS J1857+026/PSR J1856+0245 system with Fermi-LAT.

## 2. LAT description and data selection

The LAT is a gamma-ray telescope that detects photons by conversion into electron-positron pairs and operates in the energy range between 20 MeV and 300 GeV. Details of the instrument and data processing are given in Atwood et al., (2009). The on-orbit calibration is described in Abdo et al. (2009a).

The following analysis was performed using 36 months of data collected starting August 4, 2008, and extending until August, 31, 2011. Only gamma-rays in the Pass 7 Source class events were selected from this sample, we excluded those coming from a zenith angle larger than  $100^\circ$  because of the possible contamination from secondary gamma-rays from the Earth's atmosphere (Abdo et al. 2009b). We have used the P7 V6 Instrument Response Functions (IRFs). We selected the 'Source' events which correspond to a compromise between the number

<sup>1</sup> <http://www.mpi-hd.mpg.de/hfm/HESS/pages/home/sources/>

of selected photons and the background rate, following the procedure described on the Fermi Science Support Center<sup>2</sup>.

### 3. Data analysis

#### 3.1. Timing analysis of PSR J1856+0245

With its large spin-down power, the pulsar PSR J1856+0245 is one of the more energetic known radio pulsars. Its spin period of 80.9 ms and characteristic age of 20.6 kyr are similar to those of the Vela pulsar. The dispersion measure and NE2001 electron density model of the Galaxy assign PSR J1856+0245 a distance of  $\sim 9$  kpc (Cordes et al. 2002).

This pulsar is not monitored as part of the LAT pulsar timing campaign (Smith et al. 2008) but has been regularly observed with the Jodrell Bank Telescope (Hobbs et al. 2004).

The ephemeris of the pulsar PSR J1856+0245 used in the analysis of the *Fermi*-LAT data was obtained using 76 observations at 1.520 GHz made with the Jodrell Bank Telescope between 2008 May 4 and 2011 April 15. The arrival times of events were corrected to the Solar System Barycenter using the JPL DE405 Solar System ephemeris.

The TEMPO2 timing package (Hobbs et al. 2008) was then used to build the timing solution. We fit the radio times of arrival (TOAs) to the pulsar rotation frequency and first four derivatives. The post-fit rms is 1.182 ms, or 1.5 % of the pulsar phase. This timing solution will be made available through the FSSC.

Photons with energies above 100 MeV and within a radius of  $1.0^\circ$  of the pulsar radio position ( $\alpha(J2000) = 18^h56^m50.937^s$ ,  $\delta(J2000) = +02^\circ45'47.046''$ ), were selected using a energy-dependent cone of radius  $\theta_{68} < \max(5.12^\circ \times (E/100 \text{ MeV})^{-0.8}, 0.2^\circ)$  and phase-folded using the radio ephemeris previously described. This choice takes into account the instrument performance and maximizes the signal to noise ratio over a broad energy range.

The H-Test values, as defined in De Jager et al. (2009) and obtained from the pulsed analysis, correspond to a significance well below  $2\sigma$  for each tested energy band (100 MeV – 300 MeV, 300 MeV – 1 GeV, > 1 GeV). No significant pulsation is detected.

#### 3.2. Spatial and spectral analysis

Two different tools were used to perform the spatial and spectral analysis : `gtlike` and `pointlike`. `gtlike` is the maximum-likelihood method (Mattox et al. 1996) implemented in the science tools distributed by the FSSC. This tool fits a source model to the data along with models for the instrumental, extragalactic and Galactic components of the background. In the following analysis, the Galactic diffuse emission is modeled by the ring-hybrid model *gal\_2yearp7v6\_v0.fits*. The instrumental background and extra-galactic radiation are described by a single isotropic component with a spectral shape described by the tabulated model *iso\_p7v6source.txt*. The models and their description have been released by the Fermi Collaboration through the FSSC website.

`pointlike` is a binned likelihood technique that was extensively tested against `gtlike`. It convolves the intrinsic LAT PSF with a spatial model of the candidate source to create a ‘‘Pseudo-PSF’’ of the source appearance (Kerr 2011). `pointlike` can be used to assess the Test Statistic (TS) value and derive the shape and spectra of both point-like and extended sources.

The TS estimates the significance and is defined as  $TS = 2(L_1 - L_0)$  where  $L_1$  corresponds to the log-likelihood obtained by fitting a source model of the source of interest plus the background model to the data and  $L_0$  correspond to the log-likelihood obtained by fitting the background model only (Wilks 1938).

Sources in a region of  $10^\circ$  around HESS J1857+026 were extracted from the Second Fermi-LAT catalog (Abdo et al. 2011) and taken into account in this study, fixing their spectral parameters if they are more than  $5^\circ$  from our source of interest.

The region analyzed here includes the bright SNR W44, known to interact with its environment. Extended and only  $1.3^\circ$  from HESS J1857+026, W44 could influence our fit. We refitted it assuming an elliptical ring and obtained results consistent with those of Abdo et al. (2010b).

##### 3.2.1. Shape and position of the source

Source shape analysis requires the best possible angular resolution. Since the source has a hard spectrum (see Section 3.2.2) we made a compromise between statistics and resolution by selecting photons above 10 GeV. This also drastically reduces the contribution of the Galactic diffuse background. Fig. 1(b) presents a LAT TS Map in the energy range 10 GeV-100 GeV. The skymap contains the TS value for a point source at each map location, thus giving a measure of the statistical significance for the detection of a  $\gamma$ -ray source in excess of the background. A source coincident with HESS J1857+026 is clearly visible.

We determined the shape of the source using `pointlike` with three different models : a point source, a uniform disk and a Gaussian. No significant extension was obtained above 10 GeV. The best model for HESS J1857+026 is a point source located at the position  $\alpha(J2000) = 18^h57^m14.4^s$ ,  $\delta(J2000) = +02^\circ45'36.0''$  consistent with the position determined by HESS ( $\alpha(J2000) = 18^h56^m50.80^s$ ,  $\delta(J2000) = +02^\circ45'50.2''$ ).

##### 3.2.2. Spectral analysis

Fig. 1(a) shows a TS map of the region in the energy range 0.1-1.3 GeV. An emission excess appears close to HESS J1857+026. Located at ( $\alpha(J2000) = 18^h57^m19.2^s$ ,  $\delta(J2000) = +02^\circ59'13.0''$ ), this excess cannot be explained by HESS J1857+026 and was added to the model of the region.

The spectral analysis was done using `gtlike` selecting photons only between 300 MeV and 300 GeV since the low energy range is dominated by the diffuse Galactic background and subject to systematics. In this energy range, HESS J1857+026 is well described by a pure power-law with an integrated flux extrapolated down to 100 MeV of  $F(100 \text{ MeV}-100 \text{ GeV}) = (5.79 \pm 0.75 \pm 3.11) \times 10^{-9}$  ph/cm<sup>2</sup>/s, a spectral index of  $\Gamma = 1.52 \pm 0.16 \pm 0.55$  and an energy flux of  $G(100 \text{ MeV}-100 \text{ GeV}) = (2.72 \pm 0.58 \pm 1.51) \times 10^{-11}$  ergs/cm<sup>2</sup>/s leading to a significance of  $\sim 6\sigma$  (TS=38.7).

The additional background source was fitted assuming a logarithmic parabola (eq. 2 in Abdo et al. (2011)), with spectral parameters  $\alpha = 3.5 \pm 0.2_{stat}$ ,  $\beta = 0.6 \pm 0.1_{stat}$ ,  $E_0 \sim 1.2$  GeV, and  $K = (3.1 \pm 0.5_{stat}) \times 10^{-12}$  ph/MeV/cm<sup>2</sup>/s. Its significance above 300MeV is  $\sim 4.6\sigma$ .

Fermi-LAT spectral points for HESS J1857+026 were obtained by dividing the 300 MeV-300 GeV range into 4 logarithmically-spaced energy bins, as presented in Fig. 2. Both statistical and systematic errors were estimated and added in quadrature yielding the red error bars.

<sup>2</sup> FSSC: <http://fermi.gsfc.nasa.gov/ssc/data/access/lat/ephems/>

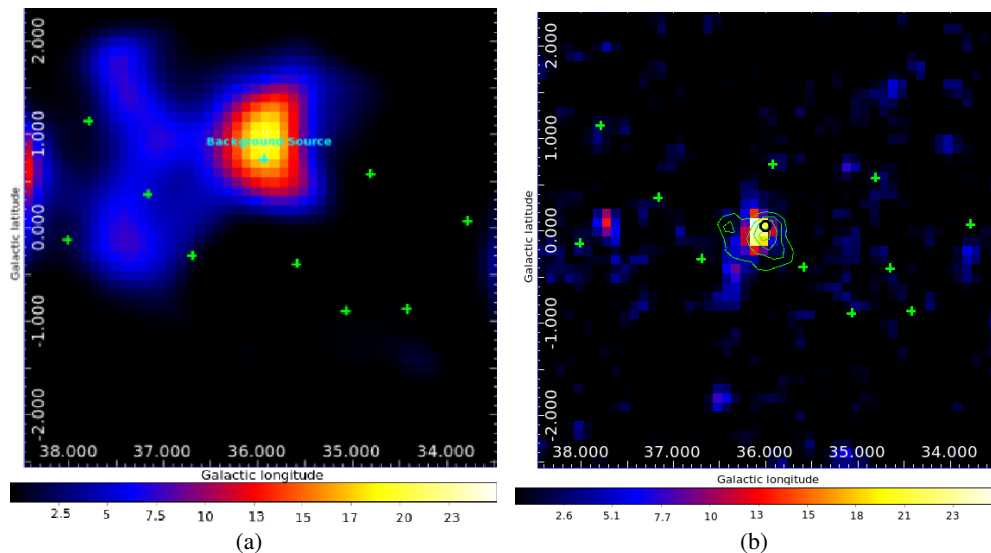


**Fig. 1.** Residual TS map obtained by fitting a source at each location of the map and computing the TS using `pointlike`. The green crosses represents the sources of the 2FGL catalog all included in the model. **(a):** Residual TS map obtained between 100 MeV and 1.3 GeV. This figure shows a residual excess taken into account in our model by adding a source to the model. **(b):** Residual TS map obtained between 10 GeV and 300 GeV. Here HESS J1857 is not included in the model. The green contours are those obtained using HESS data (Aharonian et al., 2008). The position of the Fermi excess is consistent with those of HESS. The black circle represents the position of PSR J1856+0245.

Three main systematic uncertainties can affect the LAT flux estimate for a point source: uncertainties in the Galactic diffuse background, uncertainties on the effective area and uncertainties on the shape of the source. The dominant uncertainty at low energy comes from the Galactic diffuse emission, estimated by changing the normalization of the Galactic diffuse model artificially by 6% as done in (Abdo et al., 2010). The second systematic is estimated by using modified IRFs whose effective areas bracket those of our nominal IRF as in (Grondin et al. 2011b). The fact that we do not know the true gamma-ray morphology introduces a last source of error. We derived an estimate of the uncertainty on the shape of the source by using the best Gaussian model obtained by HESS. We combine this various errors in quadrature to obtain our best estimate of the total systematic error at each energy and propagate through to the fit model parameters.

As for other PWNe detected by Fermi, HESS J1857+026 is powered by a young (Age < 21 kyrs) and energetic pulsar. Assuming a distance of 9kpc, the  $\gamma$ -ray flux obtained using Fermi-LAT data of  $L_{PWN}^{\gamma} = 2.49 \times 10^{35}$  ergs/s. This yields to a  $\gamma$ -ray efficiency of  $\sim 5\%$ . According to Fig. 7 of Ackermann et al. (2011), this is one of the highest PWN efficiencies observed in the GeV range by Fermi. It is still in the range of expected values and confirms the trend observed in the TeV band (3.1 %) using the HESS data (Mattana et al. 2009; Marandon et al. 2010).

Using our best model describing the region, we derived an upper limit on the DC emission of the pulsar. Following the procedure used by Romani et al. (2011), we added a point source at the position of the pulsar assuming a power-law of index 1.62 and a cut-off energy at 2.8 GeV. No significant signal was obtained leading to a 99% upper limit on the flux of  $6.22 \times 10^{-12}$  erg/cm<sup>2</sup>/s. Assuming a distance of 9 kpc for the pulsar, this implies a limit on the  $\gamma$ -ray luminosity of  $7.47 \times 10^{34}$  erg/s.

#### 4. Discussion

To investigate the global properties of the PWN, we apply a one-zone time dependent SED model, as described in Grondin et al.

(2011b) and Abdo et al. (2010a). This model computes SEDs from evolving electron populations over the lifetime of the pulsar in a series of time steps, with the energy content of the injected particle population varying with time following the pulsar spin down. During the free-expansion phase of the PWN (assumed to be  $\sim 10^4$  years) we adopt an expansion of  $R \propto t$ , following which the radius  $R \propto t^{0.3}$ , appropriate for a PWN expanding in pressure equilibrium with a Sedov phase SNR. Over the pulsar lifetime the magnetic field  $B \propto t^{-1.5}$ , following  $\sim 500$  years of constancy. At each time step synchrotron, inverse-Compton (Klein-Nishina effects included), and adiabatic losses are calculated. Synchrotron and IC fluxes are calculated from the final electron spectrum. We fix the pulsar braking index to the canonical value of 3, and allow the initial spin period  $P_0$  of the pulsar to vary, thereby changing the age and spin-down behavior of the pulsar.

We assume the existence of three primary photon fields (CMBR, far IR (dust), and starlight) and use the interstellar radiation mapcube within the GALPROP suite (Porter et al. 2005) to estimate the photon fields at the Galactic radius of PSR J1856+0245. A distance of 9 kpc in the direction of the pulsar corresponds to a Galactic radius of 5.4 kpc. At this radius, the peak of the SED of dust IR photons corresponds to a black body temperature of  $T \sim 32$  K with a density of  $\sim 1.1$  eV cm<sup>-3</sup>, while the SED of stellar photons peaks at  $T \sim 2500$  K with a density of  $\sim 1.2$  eV cm<sup>-3</sup>.

Spectral measurements consist of LAT, MAGIC (Klepser et al. 2011) and H.E.S.S. (Aharonian et al. 2008) data points, as well as an estimate of the X-ray flux. Hessels et al. (2008) estimate a 2–10 keV flux of  $1.6 \times 10^{-13}$  erg cm<sup>-2</sup> s<sup>-1</sup> for the faint ASCA source AX J185651+0245 coincident with the pulsar. We assign 50% error bars to this very rough estimate. Hessels et al. (2008) also estimate a non-constraining 1.4 GHz radio upper limit of  $\sim 1.8 \times 10^5$  Jy sr<sup>-1</sup>.

A simple exponentially cutoff power-law injection of electrons, evolved properly over the pulsar lifetime, often provides an adequate match to PWNe SEDS. Initially, we fit this injection spectrum with five variables: final magnetic field  $B_f =$

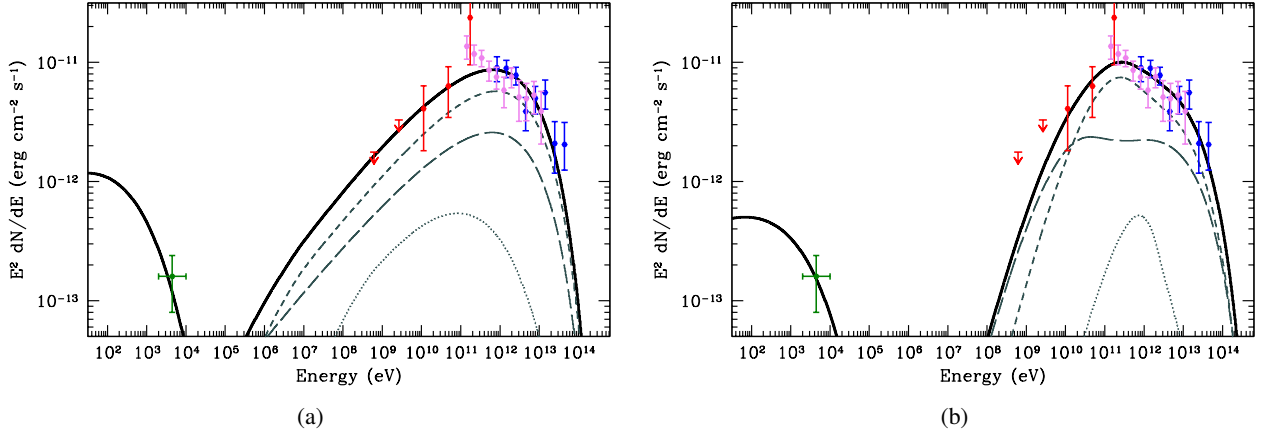


**Fig. 2.** Spectral energy distribution of HESS J1857+026 with a simple exponentially cutoff power-law electron spectrum (a), and a relativistic Maxwellian plus power-law electron spectrum (b). The X-ray flux point (green), LAT spectral points (red), MAGIC points (violet) (Klepser et al. 2011), and H.E.S.S. points (blue) (Aharonian et al. 2008) are shown. The black line denotes the total synchrotron and inverse Compton emission from the nebula. Thin curves indicate the Compton components from scattering on the CMB (long-dashed), IR (medium-dashed), and stellar (dotted) photons.

$2.1 \pm 1.0 \mu\text{G}$ , electron high energy cutoff  $E_{\text{cut}} = 59 \pm 17 \text{ TeV}$ , electron power-law index  $p = 2.15 \pm 0.03$ , initial pulsar spin period  $P_0 = 10 \pm 6 \text{ ms}$ , and pulsar braking index  $n = 3.0$ , which gives an age of 20 kyr. This simple injection spectrum yields a  $\chi^2/dof = 24.8/21$  and cannot match the low energy MAGIC points or highest energy H.E.S.S. points, as shown in Figure 2 (Top).

Another option to fit the multi-wavelength data is to adopt the relativistic Maxwellian plus power-law tail electron spectrum proposed by Spitkovsky (2008). We implement this spectrum as described in Grondin et al. (2011b). The best fit, presented in Figure 2 (Bottom), is obtained with  $kT = 0.72 \pm 0.09 \text{ TeV}$ , corresponding to an upstream gamma-factor of  $2.8 \times 10^6$ , a magnetic field of  $B_f = 1.5 \pm 0.8 \mu\text{G}$ , a cutoff at  $E_{\text{cut}} = 140 \pm 71 \text{ TeV}$  and a power-law index of  $p = 2.49 \pm 0.10$ , consistent with the value of  $\sim 2.5$  proposed by Spitkovsky (2008). The braking index of  $n = 3$  and initial spin period of  $P_0 = 42 \pm 5 \text{ ms}$  give an age of 15 kyr. The relativistic Maxwellian plus power law model better matches the multi-wavelength data, with a  $\chi^2/dof = 13.6/21$  and also directly probes the upstream pulsar wind via fitting of  $\gamma_0$ . The low magnetic field of the fit is due almost entirely to the low X-ray flux measurement, and deeper X-ray observations will hopefully improve this estimate. The MAGIC and H.E.S.S. data combine to form a power-law spectra of index  $\sim 2.3$  over nearly 3 decades in energy. This VHE data (combined with the limits imposed by the LAT data) is difficult to match with a simple power-law injection of electrons, and we find a significantly better fit with a relativistic Maxwellian plus power-law spectrum. Previous SED modeling papers have shown that in some cases the addition of a relativistic Maxwellian component improves the match between model and data (Fang et al. 2010; Slane et al. 2010; Grondin et al. 2011b).

## Acknowledgements

The Fermi-LAT Collaboration acknowledges generous ongoing support from a number of agencies and institutes that have supported both the development and the operation of the LAT as well as scientific data analysis. These include the National Aeronautics and Space Administration and the Department of Energy in the United States, the Commissariat à l’Energie

Atomique and the Centre National de la Recherche Scientifique / Institut National de Physique Nucléaire et de Physique des Particules in France, the Agenzia Spaziale Italiana and the Istituto Nazionale di Fisica Nucleare in Italy, the Ministry of Education, Culture, Sports, Science and Technology (MEXT), High Energy Accelerator Research Organization (KEK) and Japan Aerospace Exploration Agency (JAXA) in Japan, and the K. A. Wallenberg Foundation, the Swedish Research Council and the Swedish National Space Board in Sweden.

The Lovell Telescope is owned and operated by the University of Manchester as part of the Jodrell Bank Centre for Astrophysics with support from the Science and Technology Facilities Council of the United Kingdom.

## References

- A. Abdo et al., *ApJ*, 696, 2, 1084-1093, 2009 a
- A. Abdo et al., *Phys. Rev. D*, 80, 122004, 2009 b
- A. Abdo et al., *ApJ*, 713, 146, 2010 a
- A. Abdo et al., *Science*, 327, 1103-1106, 2010 b
- A. Abdo et al., *ApJS*, Submitted, 2011
- M. Ackermann et al., *ApJ*, 726, 35, 2011
- F. Aharonian et al., *A&A*, 477, 353, 2008
- W. Atwood et al., *ApJ*, 697, 2, 1071-1102, 2009
- J. Cordes, T. Lazzio, *arXiv:astro-ph/0207156*
- J. Fang, & Zhang, L. *A&A*, 515, A20, 2010
- O. De Jager et al., *A&A*, 221, 180, 1989
- B. Gaensler, P. Slane, *Ann. Rev. of A & A*, 44, 17-47, 2006.
- M.-H. Grondin, M. Lemoine-Goumard, *Heep conf., A.S.S.P.*, 399-411, 2011 a
- M.-H. Grondin et al., *ApJ*, 738, 42, 2011 b
- J.A. Hinton and W. Hofmann, *Ann. Rev. A & A*, 47, 523-565, 2010
- G. Hobbs et al., *MNRAS* 353, 1311, 2004
- G. Hobbs et al., *Chin. J. A A*, 6, 2, 189, 2006
- J. Hessels et al., *ApJ*, 682, L41L44, 2008
- M. Kerr, *arXiv:1101.6072v*
- S. Klepser et al., *proc. 32 ICRC*
- V. Marandon et al., *thesis*, 2010
- F. Mattana et al., *ApJ*, 694, 12-17, 2009
- J. Mattox et al., *ApJ*, 461, 396-407, 1996
- A. Neronov et al., *arXiv:1011.0210v1*
- A. Pellizzoni et al., *Science*, 327, 663, 2010
- T. A. Porter et al., *International Cosmic Ray Conference*, 4, 77, 2005
- R. Romani et al., *arXiv:1106.5762v1*
- P. Slane et al., *ApJ*, 720, 266, 2010
- D. Smith et al., *A&A*, 492, 3, 923-931, 2008
- A. Spitkovsky, *ApJ*, 682, L5, 2008
- D. Torres et al., *arXiv:1107.3470*

S. Wilks, Ann. Math. Stat.,9, 60, 1938

---

- <sup>1</sup> Corresponding authors : R. Rousseau (rousseau@cenbg.in2p3.fr), M. Lemoine-Goumard (lemoine@cenbg.in2p3.fr), A. Van Etten (ave@stanford.edu)
- <sup>2</sup> Université Bordeaux 1, CNRS/IN2P3, Centre d'Études Nucléaires de Bordeaux Gradignan, 33175 Gradignan, France
- <sup>3</sup> Funded by contract ERC-StG-259391 from the European Community
- <sup>4</sup> Max-Planck-Institut für Kernphysik, Saupfercheckweg 1, 69117 Heidelberg, Germany
- <sup>5</sup> Landessternwarte, Universität Heidelberg, Königstuhl, 69117 Heidelberg, Germany
- <sup>6</sup> W. W. Hansen Experimental Physics Laboratory, Kavli Institute for Particle Astrophysics and Cosmology, Department of Physics and SLAC National Accelerator Laboratory, Stanford University, Stanford, CA 94305, USA